Polymer Chemistry

ROYAL SOCIETY OF CHEMISTRY

PAPER

View Article Online
View Journal | View Issue

Cite this: *Polym. Chem.*, 2023, **14**, 1350

A systematic study on the effects of the structure of block copolymers of PEG and poly(ε-caprolactone-*co*-glycolic acid) on their temperature-responsive sol-to-gel transition behavior†

Yuichi Ohya, *[a,b] Hidenori Yonezawa,[a] Chihiro Moriwaki,[a] Nobuo Murase [c] and Akinori Kuzuya [a,b]

An aqueous polymer solution exhibiting a temperature-responsive sol-to-gel transition shows great potential as an injectable polymer (IP) system for biomedical materials. Block copolymers composed of biodegradable aliphatic polyesters and poly(ethylene glycol) (PEG) are known for their applications in medical devices. Their neat morphology and temperature responsiveness depend on their molecular structures, such as their main-chain architectures (linear or branched), block sequences, molecular weights, lengths of hydrophobic and hydrophilic segments, randomness of the hydrophobic copolymer segment, and terminal structures. However, systematic studies on the effects of these parameters have not yet been conducted. In this study, we synthesized ABA triblock, BAB triblock, and 4-arm branched block copolymers consisting of PEG as the hydrophilic segment and poly(ε-caprolactone-*co*-glycolic acid) as the hydrophobic segment with varying segment lengths, amounts of monomer (ε-caprolactone/glycolic acid) in the copolymer, and degrees of terminal modification. Their neat morphology and temperature-responsive transition behavior were analyzed. The obtained results provide molecular design guidelines for preparing biodegradable IPs that exhibit a powdery solid morphology and target-temperature gelation properties and offer the possibility of functionalization by terminal modification.

Received 17th December 2022,
Accepted 19th February 2023

DOI: 10.1039/d2py01574a

rsc.li/polymers

Introduction

Aqueous solutions of certain amphiphilic block copolymers undergo transition from a sol (colloidal) to a gel state, the so-called sol-to-gel transition, due to external stimuli such as temperature changes.[1–9] Polymers (in solution) that exhibit a sol-to-gel transition at body temperature can be used in injectable polymer (IP) systems. In particular, biodegradable thermo-gelling polymers are believed to be useful for various medical applications. Examples of these applications include less-invasive drug delivery systems providing sustained release,[10–13] anti-adhesives usable in laparoscopic operation,[14–17] cellular scaffolds for tissue regeneration and cellular therapy,[18–21] temporal embolization of blood vessels,[22–26] X-ray CT imaging[27] and endoscopic submucosal dissection (ESD).[28]

Typical examples of biodegradable thermo-gelling polymers are block copolymers of hydrophobic aliphatic polyesters and hydrophilic poly(ethylene glycol) (PEG).[1–9] Jeong *et al.*, in 1997, developed a triblock copolymer exhibiting temperature-responsive gelation.[29] The polymer has a hydrophilic–hydrophobic–hydrophilic block sequence with PEG as the hydrophilic segment and poly(L-lactic acid) (PLLA) as the hydrophobic segment (PEG–PLLA–PEG). However, the temperature-responsive transition of the polymer is gel-to-sol upon heating. Therefore, the formulation should be heated above body temperature before administration to form a hydrogel inside the body. They subsequently synthesized a triblock copolymer with a similar hydrophilic–hydrophobic–hydrophilic sequence using PEG and a random copolymer of L-lactic acid and

[a]*Department of Chemistry and Materials Engineering, Faculty of Chemistry, Materials and Bioengineering, Kansai University, 3-3-35 Yamate, Suita, Osaka 564-8680, Japan. E-mail: yohya@kansai-u.ac.jp*
[b]*Kansai University Medical Polymer Research Center (KUMP-RC), Kansai University, Suita, Osaka 564-8680, Japan*
[c]*Organization for Research and Development of Innovative Science and Technology (ORDSIT), Kansai University, Suita, Osaka 564-8680, Japan*

†Electronic supplementary information (ESI) available: Synthetic method, characterization of the polymers, typical examples of phase diagrams and rheological measurements, and supplemental plots for the relationship between polymer structure and sol-to-gel transition. See DOI: **https://doi.org/10.1039/d2py01574a**

glycolic acid (PLGA). This PEG–PLGA–PEG block copolymer shows a sol-to-gel transition upon heating.[30–32] These hydrophilic–hydrophobic–hydrophilic sequence polymers (PEG–PLLA–PEG and PEG–PLGA–PEG) were synthesized by coupling reactions of the respective AB-type diblock copolymers (PEG–PLLA or PEG–PLGA). In 2001, Lee *et al.* reported a triblock copolymer with a reversed sequence of hydrophobic–hydrophilic–hydrophobic (referred to as the ABA-type hereafter), consisting of PLGA (A segment) and PEG (B segment) exhibiting a sol-to-gel transition upon heating.[33] The ABA-type block copolymers have an advantage in the preparation process: PLGA–PEG–PLGA can be synthesized in one pot by copolymerizing lactide (LA) and glycolide (GL) using PEG as the macroinitiator. PLGA–PEG–PLGA has been recognized as ReGel®, and the applications of the copolymer in drug delivery devices have been studied widely.[34–36] However, the neat morphology of the PLGA-based thermo-gelling block copolymers, including ReGel®, forms a sticky paste at room temperature (r.t.) in the dry state, making it difficult to handle. Moreover, it takes several hours to dissolve these polymers in water.

After the pioneering studies described above, ABA- or BAB-type triblock copolymers consisting of PEG and various aliphatic polyesters, such as poly(ε-caprolactone) (PCL),[37–41] PLGA,[42–44] poly(ε-caprolactone-*co*-glycolide) (PCGA),[45–47] and PLLA/PDLA stereocomplexes,[48,49] have been developed as thermo-gelling copolymer systems. PCL is a semi-crystalline polymer with a relatively low melting point (~60 °C). Block copolymers consisting of PCL as the hydrophobic segment show a powdery morphology at r.t. in the dry state.[37–41] However, it is necessary to heat the block copolymers above their melting temperatures (50–60 °C) to dissolve them in aqueous solutions. Moreover, aqueous solutions of the PCL-based block copolymers tended to spontaneously transform into a hydrogel or precipitate after a certain period at r.t. or lower temperatures because of the high crystallinity of PCL segments.[41] Deng *et al.* reported the influence of crystallinity of the hydrophobic segment on the morphology of thermo-gelling block copolymers.[46] Then, Ding *et al.* found that the issue of insolubility could be solved by copolymerization of ε-caprolactone (CL) with GL and reducing the crystallinity of hydrophobic segments using a triblock copolymer of PCGA and PEG (PCGA–PEG–PCGA).[47] By freeze-drying aqueous solutions of the block copolymer, cotton-like solids could be obtained, which could be quickly dissolved in water.[47,50] We also studied the functionalization of PCGA–PEG–PCGA copolymer systems and their application in biomedical materials.[51–54]

On the other hand, thermo-gelling copolymer systems with various main-chain architectures, such as star-shaped branched block copolymers,[19,55–59] graft copolymers,[60–64] and multi-block copolymers,[65] have been reported in other studies. The sol-to-gel transition of thermo-gelling copolymer systems consisting of PEG is triggered by the dehydration of the PEG segment upon heating. The dehydration temperature of PEG strongly depends on its chain length. Therefore, such variations in the main-chain architecture (branched, graft, or multi-block) can provide a divided arrangement of PEG segments in one macromolecule and contribute to the increase in total molecular weight (MW) of the polymers while maintaining the hydrophobic/hydrophilic segment ratio. This may improve the mechanical properties in the gel state. It is known from empirical knowledge that a shorter PEG and a longer hydrophobic segment, *i.e.*, a higher hydrophobic/hydrophilic segment ratio, leads to a lower gelation temperature (T_{gel}). We reported that a graft-type polylactide copolymer with shorter PEG graft chains had a lower T_{gel} than that with longer PEG graft chains, even though they had the same PEG content.[63] Then we succeeded in obtaining a graft copolymer with larger MWs while maintaining the desired T_{gel}.

Moreover, the hydrophobicity (or hydrophilicity) of the termini of thermo-gelling polymers significantly influences the sol-to-gel transition. Block copolymers with hydrophobic (aliphatic polyester) outer segments usually carry hydrophilic hydroxyl groups at their termini, which are the chain ends of ring-opening polymerization. We found that the T_{gel} of PCGA–PEG–PCGA decreased after converting the terminal hydroxyl groups to acryloyl ester groups because of the increase in hydrophobicity.[66]

As described above, the block sequence (ABA or BAB), main-chain architecture (linear or branched), constituent monomers, length of each segment (hydrophobic/hydrophilic segment ratio), crystallinity of the hydrophobic segments, and structures of terminal groups (hydrophilic or hydrophobic) have a great influence on the neat morphology and temperature-responsive phase transition behavior of the polymers. However, only a few systematic studies on the effects of the molecular structure of thermo-gelling polymers (particularly PCGA-based polymers) on such properties have been conducted in detail.[67,68] In this study, we prepared ABA- and BAB-type triblock copolymers of PCGA (A segment) and PEG (B segment) with various PCGA chain lengths, monomer compositions (CL to glycolic acid (GA) ratios, CL/GA), and degrees of substitution (DS) of acetyl or butyryl groups at the termini (Fig. 1). Moreover, we synthesized 4-arm branched block copolymers (4-arm PEG–PCGA) by ring-opening copolymerization of CL and GL, using 4-arm branched PEG as the macroinitiator. The hydroxyl termini of the obtained 4-arm PEG–PCGA were acetylated to various degrees. Then, the temperature-responsive phase transition (typically sol-to-gel) behavior and neat morphology of the obtained polymers were determined. Finally, the relationship between the molecular structure and these properties is discussed systematically.

Experimental

Synthesis of the polymers

Several series of block copolymers with linear or 4-arm branched structures, different block sequences (ABA or BAB) with different lengths and CL/glycolic acid (GA) ratios of PCGA segments (GL corresponds to two GA units), and different degrees of terminal modifications were successfully syn-

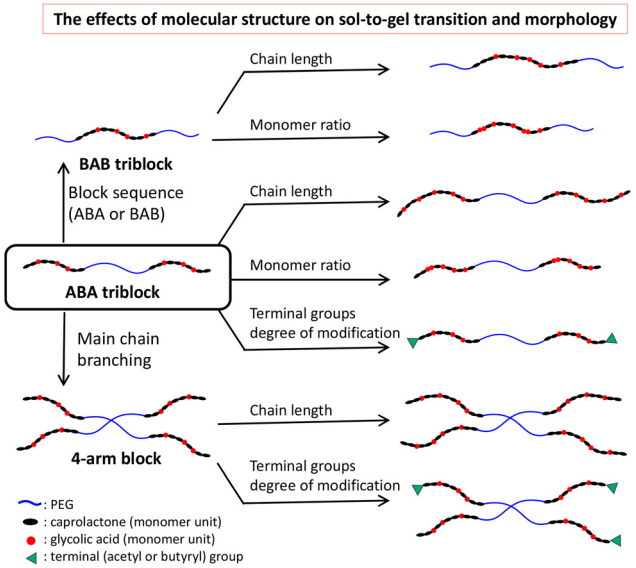

Fig. 1 Schematic illustration of the concept of this study: the effects of the molecular structure on sol-to-gel transition and morphology.

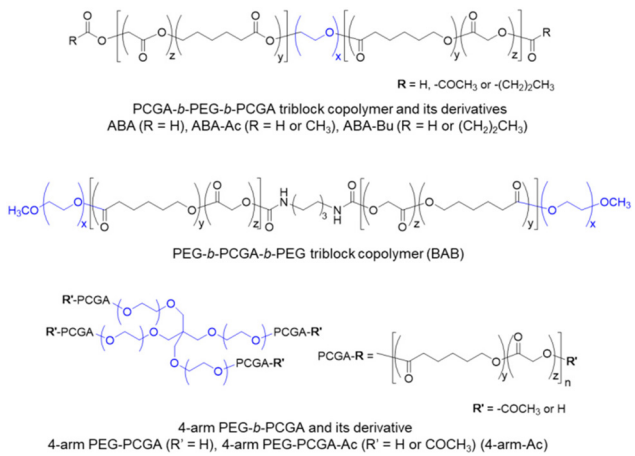

Fig. 2 Molecular structures of the polymers used in this study.

thesized using methods similar to those reported previously.[50,51] Fig. 2 shows the molecular structures of the polymers used in this study. The results of the characterization of ABA triblock copolymers are summarized in Table 1 as typical examples. The details of the synthesis methods and characterization of the other polymers are described in the ESI (Schemes S1–S4, Fig. S1–S6 and Tables S1–S4†).

ABA triblock copolymers (PCGA–PEG–PCGAs) with different PEG lengths (MW = 1000, 1540 or 2000 g mol^{-1}), PCGA lengths (MW = 900–2300 g mol^{-1}), and CL/GA ratios (1.6–6.1) were prepared by ring opening copolymerization of CL and GL using PEG as the macroinitiator. The polymer structures are listed in Table 1. We used code names to represent each ABA-type copolymer, for example, ABA1.5k–2.4k–3.6, where 1.5k = MW of a PEG segment, 2.4k = sum of MWs of two PCGA segments, and 3.6 = molar ratio of CL/GA in the PCGA segments.

AB diblock copolymers (PEG–PCGAs) with one hydroxyl terminal were obtained by ring-opening polymerization of CL and GL using mono-methoxy-PEG (MeO-PEG$_{550}$, MW = 550) as the macroinitiator. BAB triblock copolymers (PEG–PCGA–PEGs) were synthesized by dimerization of the available PEG–PCGAs using hexamethylene diisocyanate (HMDI). The characteristics of the BAB triblock copolymers are summarized in Table S1.† PEG–PCGA–PEG with various PCGA lengths (MW = 2100–5600 g mol^{-1}) and CL/GA ratios (1.5–4.7) were obtained. We used code names to represent each BAB-type copolymer, for example, BAB1.1k–2.1k–2.4, where 1.1k = sum of MWs of two PEG segments, 2.1k = total MW of PCGA as the middle segment (two PCGA segments connected with a hexamethylene spacer and urethane bonds), and 2.4 = molar ratio of CL/GA in the PCGA segment.

PCGA–PEG–PCGA (ABA) triblock copolymer derivatives with different DS of terminal acetyl or butyryl groups (ABA-Ac and ABA-Bu series) were synthesized using an ABA triblock copolymer (ABA1.5k–3.1k–3.4) and acetic acid anhydride or butyric acid anhydride. The characterization of the ABA-Ac and ABA-Bu series polymers is summarized in Table S2.† We used code names to represent each terminus-modified copolymer, such as ABA-Ac$_{22}$ or ABA-Bu$_{12}$, where 22 and 12 represent the DS of acetyl or butyryl groups (%), respectively. As a result, the ABA-Ac series with various DS (22.3–95.8%) and the ABA-Bu series with various DS (12.0–91.3%) were obtained.

4-Arm PEG–PCGA derivatives (4-arm series) with different PCGA lengths (MW = 900 × 4–5000 × 4 g mol^{-1}) and similar CL/GA ratios (3.2–4.1) were also synthesized (Table S3†). We used code names to represent each 4-arm copolymer, for example, 4-arm5.0k–3.6k, where 5.0k = MW of the 4-arm PEG used and 3.6k = total MW of four PCGA segments (900 × 4 g mol^{-1}). 4-Arm PEG–PCGA derivatives with different DS of terminal groups with acetyl groups (4-arm-Ac series) were also synthesized using 4-arm PEG–PCGA (4-arm5.0k–7.6k) using the same method. We used code names to represent the 4-arm-Ac series, such as 4-arm-Ac$_{18}$, where 18 = DS of acetyl groups (%). As shown in Table S4,† the 4-arm-Ac series with various DS (17.5–94.7%) were obtained.

We investigated the neat morphology of all the obtained polymers. Fig. 3 shows the photographs of three representative ABA and BAB triblock copolymers, each displaying powdery solid, sticky solid, and viscous liquid morphologies. Photographs of other polymers are shown in the ESI (Fig. S7–S12†). Typical examples of phase diagrams (sol, gel, or precipitate states as functions of temperature and polymer concentration) and temperature-dependent dynamic rheological measurements are shown in Fig. S13 and S14 in the ESI,† respectively.

Results and discussion

Morphology and gelation behavior of ABA and BAB triblock copolymers

The morphology, transition modes, and temperatures of the ABA and BAB-type copolymers are shown in Tables 1 and S1.†

Table 1 Characterization of the PCGA–PEG–PCGA triblock copolymers (ABA series)

Code	MW of PEG[a] (g mol^{-1})	MW of PCGA[b] (g mol^{-1})	CL/GA[c] (mol/mol)	Total M_n[d] (g mol^{-1})	M_w/M_n[e]	PCGA%[f]	Morphology	T_{gel}[g] (°C)	Temperature for other transition[h] (°C)
ABA1.5k–2.4k–3.6	1540	1200 × 2	3.6	3940	1.4	60.9	Sticky solid	N.D.	57[i]
ABA1.5k–3.0k–3.5		1500 × 2	3.5	4540	1.4	66.1	Sticky solid	45	48[i]
ABA1.5k–3.1k–3.4		1550 × 2	3.4	4640	1.3	66.8	Powdery solid	42	45[k], 53[i]
ABA1.5k–3.2k–3.6		1600 × 2	3.6	4740	—	67.5	Powdery solid	44	52[j]
ABA1.5k–3.5k–3.4		1750 × 2	3.4	5040	1.3	66.9	Powdery solid	38	47[k], 55[i]
ABA1.5k–3.6k–4.8		1800 × 2	4.8	5140	1.4	70.0	Powdery solid	34	52[j]
ABA1.5k–3.6k–5.5		1800 × 2	5.5	5140	1.6	70.0	Powdery solid	34	53[j]
ABA1.5k–3.8k–3.1		1900 × 2	3.1	5340	1.6	71.2	Powdery solid	33	54[j]
ABA1.5k–3.8k–3.5		1900 × 2	3.5	5340	1.3	71.2	Powdery solid	33	47[j]
ABA1.5k–3.8k–6.1		1900 × 2	6.1	5340	—	71.2	Powdery solid	34	50[j]
ABA1.5k–3.9k–1.6		1950 × 2	1.6	5440	—	71.7	Viscous liquid	30	49[j]
ABA1.5k–4.0k–3.7		2000 × 2	3.7	5540	1.5	72.2	Powdery solid	33	50[j]
ABA1.5k–4.6k–3.5		2300 × 2	3.5	6140	1.5	74.9	Powdery solid	— (insoluble)	— (insoluble)
ABA1.0k–1.8k–3.9	1000	900 × 2	3.9	2800	1.4	64.4	Sticky solid	N.D.	51[i]
ABA1.0k–2.0k–3.7		1000 × 2	3.7	3000	—	66.7	Sticky solid	N.D.	51[i]
ABA1.0k–2.0k–4.1		1000 × 2	4.1	3000	1.5	66.7	Sticky solid	N.D.	52[j]
ABA1.0k–2.6k–3.6		1300 × 2	3.6	3600	1.5	72.2	Sticky solid	13	21[k]
ABA1.0k–3.0k–3.4		1500 × 2	3.4	4000	—	75.0	Sticky solid	11	—
ABA2.0k–4.6k–2.7	2000	2300 × 2	2.7	6600	1.5	69.7	Powdery solid	56	64[k], 67[j]

[a] As indicated by the supplier. [b] Estimated by ^{1}H-NMR. [c] Molar ratios of CL to GA found in the polymer, estimated by ^{1}H-NMR. [d] Number-average molecular weight estimated by ^{1}H-NMR. [e] Polydispersity index estimated by size exclusion chromatography (SEC). [f] Weight content of the PCGA segment = [(MW of the total polymer) − (MW of the PEG unit)]/(MW of the total polymer) × 100 (%). [g] Sol-to-gel transition temperature determined by the test tube inversion method. [h] Transition temperature for other than sol-to-gel transition, shown in (i)–(k). [i] Sol-to-precipitate transition. [j] Gel-to-precipitate transition. [k] Gel-to-sol transition. N.D.: not detected, —: not determined.

The results for all ABA and BAB series are summarized in Fig. 4, which is a plot on the 2-dimensional *X*–*Y* plane with the CL/GA ratio as the *X*-axis and the MW of the PCGA segments as the *Y*-axis. In this figure, the shapes of the symbol represent the neat morphology of the polymer at r.t. and in the dry state: circles represent powdery solids, triangles and diamonds indicate sticky solids, and squares represent viscous liquids. The phase transition modes with increasing temperature are represented by the colors of the symbols: red indicates sol-to-gel transition, and the others do not exhibit sol-to-gel transition. Green indicates the transition from a turbid sol to precipitate, and blue indicates the transition from a transparent sol to precipitate. Black indicates insolubility, which makes it impossible to determine the transition point. For each symbol, closed and open symbols represent the ABA or BAB block sequences, respectively.

Besides ABA2.0k, the polymers showing powdery solid morphologies were found in the region of MW of PCGA ≥ 3.1k and CL/GA ratio ≥ 3.1 (yellow square in Fig. 4). Outside this region, the morphology became a sticky solid and viscous liquid. It was difficult to determine a clear boundary between the viscous liquid and sticky solid states because of the low number of plot points. This is also tentatively indicated in light blue with a dotted line.

In contrast, the red symbols showing polymers exhibiting sol-to-gel transition are distributed in the area where the MW of PCGA is between 2.9k and 4.2k (indicated in pale red), regardless of the CL/GA ratio. Only two red plots were located outside this area, ABA1.0k and ABA2.0k using PEG with MWs = 1000 (ABA1.0k–2.6k–3.6) and 2000 (ABA2.0k–4.6k–2.7), respectively. The T_{gel} values of these polymers are 13 °C and 56 °C (Table 1). Because these are much lower than r.t. or higher than body temperature, the polymers do not substantially gel around r.t. and body temperature, and these can be treated as outliers. However, only MeO-PEG (MW = 550) was used for the outer (hydrophilic) segments of the BAB series in this study. Therefore, it is possible that the trends observed in this plot will not apply to different chain lengths of MeO-PEG. These results suggest that the CL/GA ratio strongly influences the morphology of ABA and BAB block copolymers. However, the effect of MW of the PCGA segment is more dominant than that of the CL/GA ratio in determining whether the transition mode is a sol-to-gel transition. It is confirmed that the ratio of the hydrophobic component greatly contributes to the gelation behavior.

An alternative plot using the hydrophobic segment/hydrophilic segment ratio instead of the MW of PCGA is shown in Fig. S15 (ESI).† PCGA% is used as a parameter for the hydrophobic/hydrophilic segment ratio and is determined using the following equation:

$$\mathrm{PCGA\%} = \frac{(\text{MW of total polymer}) - (\text{MW of PEG})}{(\text{MW of total polymer})} \times 100$$

In this plot based on PCGA%, PEG2.0k, which is an outliner in Fig. 4, seems to fall in an appropriate place. Although other basic trends are similar to those observed in Fig. 4, overlaps of

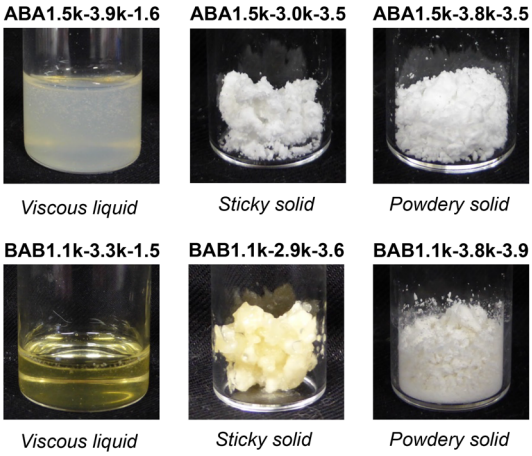

Fig. 3 Photographs of representative ABA and BAB triblock copolymers showing powdery, sticky solid and viscous liquid morphologies.

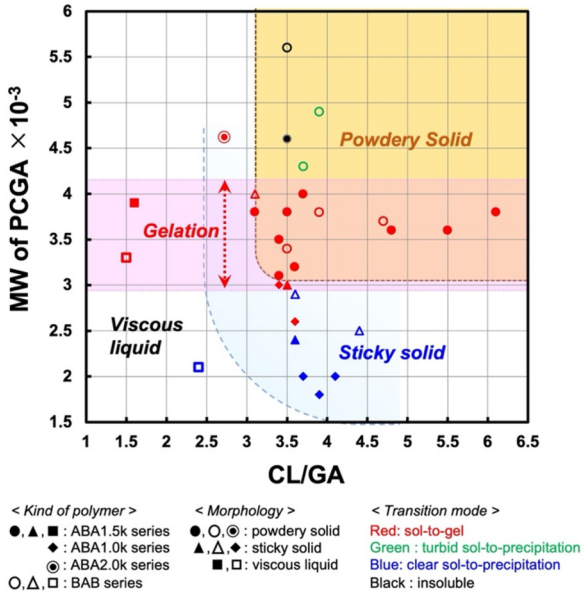

Fig. 4 Effects of MW of PCGA and CL/GA ratios on the morphology and transition modes of linear block copolymers. Closed circle, triangle, and square: ABA1.5k series (MW of PEG = 1540), closed diamond: ABA1.0k series (MW of PEG = 1000), double circle: ABA2.0k (MW of PEG = 2000), and open symbols: BAB series. Circle: powdery solid, triangle and diamond: sticky solid, and square: viscous liquid. Red: sol to gel, green: turbid sol to precipitate, blue: clear sol to precipitate, and black: insoluble.

some of the different characteristic symbols are observed and it is difficult to determine the boundaries of regions in Fig. S15.†

To study the effects of the hydrophobic/hydrophilic ratio (PCGA%) on T_{gel} in more detail, only the ABA- and BAB-type copolymers exhibiting sol-to-gel transition were plotted against PCGA% in Fig. 5. It was confirmed that T_{gel} decreases with increasing PCGA% for all ABA1.5k, ABA1.0k, and BAB series. There is relatively good linearity for the decrease in T_{gel} *vs.* % PCGA in the results of the ABA1.5k series. Although such linearity is not clear for the ABA1.0k series and BAB series because of the small number of plots and the variation in values, it is promising for the ABA1.5k series. Despite such tendencies, T_{gel} decreases with an increase in the hydrophobic component ratio, as stated in many previous reports,[33,36,38,46] and such a linear relationship has not been clearly shown. Our study revealed a linear relationship between T_{gel} and the hydrophobic component ratio in an ABA triblock copolymer system.

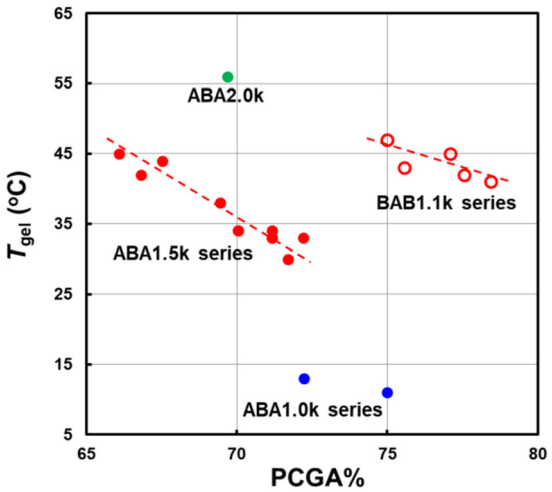

Fig. 5 Relationship between gelation temperature (T_{gel}) and weight content of the PCGA segment (PCGA%) for ABA and BAB triblock copolymers. Closed red circle: ABA1.5k series (MW of PEG = 1540), closed blue circle: ABA1.0k series (MW of PEG = 1000), closed green circle: ABA2.0k (MW of PEG = 1000), and open red circle: BAB series.

Regarding the length of the PEG chain for ABA block copolymers, comparing ABA1.0k–2.6k–3.6, ABA1.5k–3.6k–ABA1.5k–3.9k, and ABA2.0k–4.6k–2.7 with similar PCGA% (71 ± 1.3%), polymers with a longer PEG chain showed a higher T_{gel}. This is because the dehydration temperature of PEG strongly depends on the MW,[69] and the results are in good agreement with our previous report on graft copolymers.[63] Fig. S16 (ESI†) shows the relationship between the T_{gel} and the CL/GA ratio of the ABA1.5k and BAB series with a MW similar to that of PCGA (3.3k–4.0k). The T_{gel} was almost constant regardless of the CL/GA ratio (Fig. S16†). Differential scanning calorimetry (DSC) was used to analyze some of the ABA1.5k and BAB series to investigate the relationship between crystallinity and T_{gel} (Table S5 and Fig. S17†). However, we did not find clear trends other than those already described in Fig. 4, 5 and S16.† This might be because a small number of samples was measured; however, PCGA% is more dominant than crystallinity in the range of measurements. As discussed above, along with Fig. 4, it was clarified that the CL/GA ratio, that is, the crystallinity of the hydrophobic segment, affects the morphology but not the transition temperature.

The effect of terminal groups on the gelation behavior of ABA-type triblock copolymers

Next, we investigated the change in T_{gel} of the ABA1.5k copolymers due to acetylation and butyrylation at the termini with

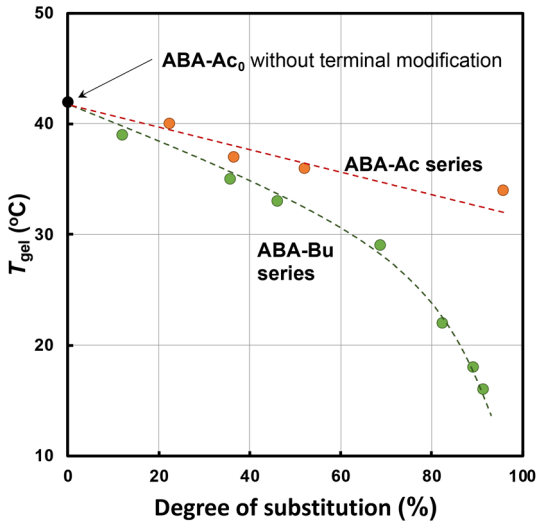

Fig. 6 Effect of the degree of substitution (DS) (%) of terminal groups with acetyl or butyryl groups on the gelation temperature (T_{gel}) of ABA triblock copolymers. ABA1.5k–3.1k–3.4 was used as the base polymer (ABA-Ac_0) for terminal modifications. Orange: acetyl, green: butyryl, and black: base polymer (ABA-Ac_0 = ABA1.5k–3.1k–3.4) without modification.

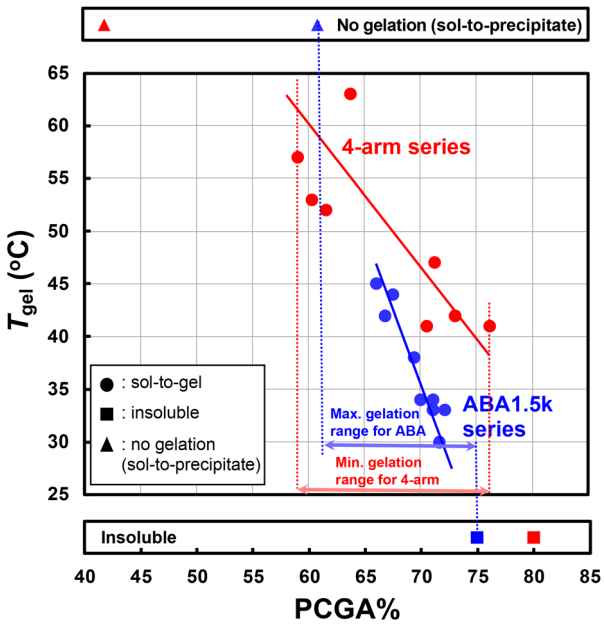

Fig. 7 Comparison of the effect of PCGA% on gelation temperature (T_{gel}) for linear ABA triblock and 4-arm branched PEG–PCGA copolymers. Circle: sol-to-gel transition, triangle: no gelation (sol to precipitation), and square: insoluble. Blue: ABA1.5k series (MW of PEG = 1540) and red: 4-arm PEG–PCGA series.

different DS (ABA-Ac and ABA-Bu series) (Fig. 6 and Table S2†). Almost all the samples were powdery solids. The structure and DS of the terminal groups in these polymers did not significantly affect the morphology. The T_{gel} decreases linearly with increasing DS of acetyl groups. The difference in T_{gel} between ABA-Ac_{96} (DS = 96%) and the original polymer (ABA-Ac_0 = ABA1.5k–3.1k–3.4) is 8 °C. On the other hand, the decrease in T_{gel} is greater with increasing DS of the more hydrophobic butyryl group. The difference in T_{gel} between ABA-Bu_{91} (DS = 91%) and the original polymer (ABA-Ac_0 = ABA1.5k–3.1k–3.4) is 26 °C. The differences between the ABA-Ac and ABA-Bu series are small at the lower DS region (<50%), but significantly larger in the higher DS region. These results suggest that the remaining terminal hydroxyl groups are dominant in lower DS regions. In comparison, the increase in terminal hydrophobicity has a more remarkable influence on T_{gel} in higher DS regions.

Comparison of branched (4-arm) and linear ABA block copolymers

To investigate the effect of the branched structure of the main chain on gelation behavior, we compared 4-arm PEG–PCGA (4-arm series) with the linear ABA1.5k series concerning varying PCGA% (Fig. 7 and Table S3†). Only two samples with short PCGA chains (4-arm5.0k–3.6k and 4-arm5.0k–7.2k) show a sticky solid morphology. However, the others show a powdery solid morphology. In the 4-arm series, the influence of PCGA% on the morphology is not so significant.

The T_{gel} of the 4-arm series also decreases with increasing PCGA%. However, the slope for the ABA1.5k series is greater than that for the 4-arm series. Although the PCGA% ranges where gelation occurs overlap, the 4-arm series exhibit sol-to-gel transition in a wider PCGA% range than the ABA1.5k series. ABA1.5k–4.6k–3.5 with PCGA% = 75% is insoluble, but 4-arm5.0k–16.0k with a similar PCGA% = 76% is soluble and exhibits gelation. A similar observation can be made in the lower boundary, where ABA1.5k–2.4k–3.6, with PCGA% = 61%, did not show sol-to-gel transition (sol-to-precipitate), but 4-arm5.0k–7.2k with lower PCGA% = 59% exhibits sol-to-gel transition. In other words, the gelation range for the 4-arm series is at least between 59 and 76 PCGA% (indicated with the red double-headed arrow), which is larger than the gelation range (at most) for the linear ABA series between 61 and 75 PCGA% (indicated with the blue double-headed arrow). A similar trend is observed in Fig. S18 in the ESI,† where the same data are plotted against the MW of one PCGA segment for each copolymer. The MW range of a PCGA showing gelation spans 1500–2000 g mol^{-1} for the ABA series and 1800–4000 g mol^{-1} for the 4-arm series, while the temperature range spans 15 °C (30 °C–45 °C) for the ABA series and 16 °C (41 °C–57 °C) for the 4-arm series, respectively. All plots for the ABA series were close to the approximation line, showing good linearity. However, the 4-arm series plots deviate significantly from the approximation line. The influence of polydispersity of the polymers on the gelation behavior has been reported in the literature.[70,71] Therefore, the significant deviation observed may be due to the relatively wide distribution of the polydispersity index (M_w/M_n) for the 4-arm series (ranging from 1.5 to 2.2), and the difficulty in accurately determining the total number average molecular weight, M_n, for branched copolymers.

According to these results, a small difference in the MW of PCGA resulted in a relatively large change in the T_{gel} of linear ABA triblock copolymers. Therefore, it is necessary to control the degree of polymerization of the PCGA chain precisely during synthesis to obtain a polymer with the targeted T_{gel}. This should not be difficult to control if the intended polymerization is successful owing to the relatively linear relationship between the MW of PCGA and the T_{gel} value. Conversely, the tolerance range for the PCGA chain length for sol-to-gel transition behavior may be wider for 4-arm PEG–PCGA, but a highly accurate target T_{gel} is difficult to obtain.

Finally, we synthesized 4-arm PEG–PCGA with various DS of acetyl groups at the termini (4-arm-Ac series, Table S4†), using 4-arm5.0k–7.6k as the original polymer. The 4-arm-Ac series with a moderate DS of acetyl groups showed a sticky solid morphology, although the original polymer (4-arm-Ac_0) and the 4-arm-Ac series with high or low DS of acetyl groups (4-arm-Ac_{18} and 4-arm-Ac_{95}) showed a powdery solid morphology. This may be because different terminal groups (–OH or –$OCOCH_3$) in a molecule inhibited the crystal formation of the PCGA segments in the neat polymer. Fig. 8 shows the comparison of the effects of terminal acetyl group modifications of the 4-arm-Ac and ABA-Ac (the same data shown in Fig. 6) series on their T_{gel}. Although the temperature ranges of T_{gel} in these two datasets were different, they exhibited very similar trends. T_{gel} decreases linearly with increasing DS of the acetyl groups, and the slopes were almost the same. These results suggest that the contribution of the degree of terminal modification with acetyl groups is approximately the same for both the linear ABA triblock copolymer and the 4-arm PEG–PCGA.

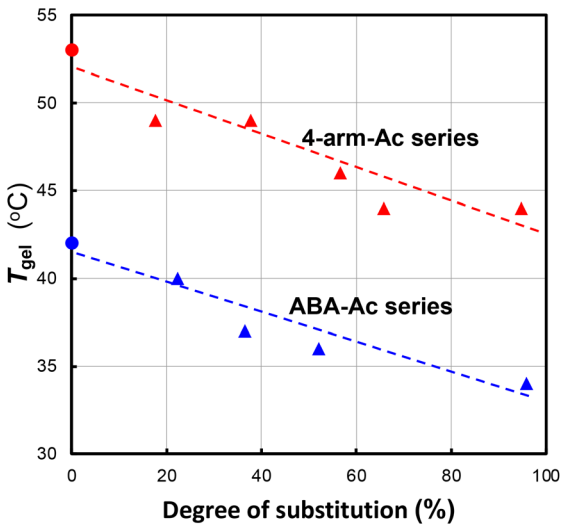

Fig. 8 Effect of the degree of substitution (DS) (%) with acetyl groups on the gelation temperature (T_{gel}) for linear ABA triblock (ABA-Ac series, the same data are shown in Fig. 5, blue) and 4-arm branched PEG–PCGA copolymers (4-arm-Ac series, red). For the 4-arm-Ac series, 4-arm5.0k–7.6k (4-arm-Ac_0) was used as the base polymer for terminal modifications.

Conclusions

We synthesized various linear ABA triblock, BAB triblock, and 4-arm block copolymers consisting of PCGA (A segment) and PEG (B segment) with different MWs of PCGA segments, CL/GA ratios, and DS of acetyl or butyryl groups on their terminal groups. We then investigated the effects of the molecular structures on the neat morphologies and gelation behavior. Both ABA and BAB linear triblock copolymers exhibit a powdery solid morphology when the CL/GA and PCGA chain lengths exceed a certain range. The CL/GA ratio, which determines the crystallinity of the PCGA segment, influences the morphology of the linear block copolymers. However, it does not have a significant influence on T_{gel}. The PCGA chain length (the content of the hydrophobic segment) has a greater effect on the sol-to-gel transition. The T_{gel} of the linear ABA triblock copolymers was more sensitive to the length of the hydrophobic (PCGA) segment than that of the 4-arm PEG–PCGA system. Good linearity for T_{gel} and hydrophobic segement content (%PCGA) was observed for the ABA linear triblock copolymers. The substitution of terminal hydroxyl groups with acetyl or butyryl groups lowered the T_{gel}, where the decrease in T_{gel} was more drastic for the butyryl than the acetyl groups owing to their higher hydrophobicity. There was no significant difference in the effect of terminal group modification with acetyl groups between the linear ABA triblock copolymer and 4-arm PEG–PCGA systems. These results provide a molecular design guideline for synthesizing biodegradable injectable polymers that exhibit a powdery morphology and gelation at a target temperature and a means for functionalization by terminal modification.

Author contributions

Y. O. designed and supervised the experiments. H. Y. and C. M. performed the experiments. N. M. and A. K. performed some of the measurements and analyzed the data. Y. O. prepared the manuscript. All authors have discussed the results.

Conflicts of interest

There are no conflicts to declare.

Acknowledgements

This work was financially supported in part by the Private University Research Branding Project with matching fund subsidies from the Ministry of Education, Culture, Sports, Science, and Technology (MEXT), Japan (2016–2020), and Grants-in-Aid for Scientific Research (16H01854 and 20H00670) from the Japan Society for the Promotion of Science (JSPS). The authors thank NOF Co. for providing 4-arm PEG.

References

1 L. Yu and J. Ding, *Chem. Soc. Rev.*, 2008, **37**, 1473.
2 M. K. Nguyen and D. S. Lee, *Macromol. Biosci.*, 2010, **10**, 563.
3 C. T. Huynh, M. K. Nguyen and D. S. Lee, *Macromolecules*, 2011, **44**, 6629.
4 Y. Li, J. Rodrigues and H. Tomas, *Chem. Soc. Rev.*, 2012, **41**, 2193.
5 K. Nagahama, A. Takahashi and Y. Ohya, *React. Funct. Polym.*, 2013, **73**, 979.
6 A. P. Mathew, S. Uthaman, K. H. Cho, C. S. Cho and I. K. Park, *Int. J. Biol. Macromol.*, 2018, **110**, 17.
7 M. H. Park, M. K. Joo, B. G. Choi and B. Jeong, *Acc. Chem. Res.*, 2012, **45**, 424.
8 H. J. Moon, D. Y. Ko, M. H. Park, M. K. Joo and B. Jeong, *Chem. Soc. Rev.*, 2012, **41**, 4860.
9 J. Shi, L. Yu and J. Ding, *Acta Biomater.*, 2021, **128**, 42.
10 S. Choi, M. Baudys and S. W. Kim, *Pharm. Res.*, 2004, **21**, 827.
11 K. Manokruang and D. S. Lee, *Macromol. Biosci.*, 2013, **13**, 1195.
12 K. Li, L. Yu, X. Liu, C. Chen, Q. Chen and J. Ding, *Biomaterials*, 2013, **34**, 2834.
13 Y. Wang, X. Yang, X. Chen, X. Wang, Y. Wang, H. Wang, Z. Chen, D. Cao, L. Yu and J. Ding, *Adv. Funct. Mater.*, 2022, **32**, 2206554.
14 Z. Zhang, J. Ni, L. Chen, L. Yu, J. Xu and J. Ding, *Biomaterials*, 2011, **32**, 4725.
15 L. Yu, H. Hu, L. Chen, X. Bao, Y. Li, L. Chen, G. Xu, X. Ye and J. Ding, *Biomatr. Sci.*, 2014, **2**, 1100.
16 J. H. Hong, J. W. Choe, G. Y. Kwon, D. Y. Cho, D. S. Sohn, S. W. Kim, Y. C. Woo, C. J. Lee and H. Kang, *J. Surg. Res.*, 2011, **166**, 206.
17 Y. Yoshizaki, T. Nagata, S. Fujiwara, S. Takai, D. Jin, A. Kuzuya and Y. Ohya, *ACS Appl. Bio Mater.*, 2021, **4**, 3079.
18 B. Yeon, M. H. Park, H. J. Moon, S. J. Kim, Y. W. Cheon and B. Jeong, *Biomacromolecules*, 2013, **14**, 3256.
19 K. Nagahama, T. Ouchi and Y. Ohya, *Adv. Funct. Mater.*, 2008, **18**, 1220.
20 N. Oyama, H. Minami, D. Kawano, M. Miyazaki, T. Maeda, K. Toma, A. Hotta and K. Nagahama, *Biomater. Sci.*, 2014, **2**, 1057.
21 Y. Yoshizaki, M. Ii, H. Takai, N. Mayumi, S. Fujiwara, A. Kuzuya and Y. Ohya, *Sci. Technol. Adv. Mater.*, 2021, **22**, 627.
22 P. Kan, X. Z. Lin, M. F. Hsieh and K. Y. Chang, *J. Biomed. Mater. Res., Part B*, 2005, **75**, 185.
23 X. Chen, L. Huang, H. J. Sun, S. Z. D. Cheng, M. Zhu and G. Yang, *Macromol. Rapid. Commun.*, 2014, **35**, 579.
24 H. Yang, K. Lei, F. Zhou, X. Yang, Q. An, W. Zhu, L. Yu and J. Ding, *Mater. Sci. Eng., C*, 2019, **102**, 606.
25 L. Weng, N. Rostambeigi, N. D. Zantek, P. Rostamzadeh, M. Bravo, J. Carey and J. Golzarian, *Acta Biomater.*, 2013, **9**, 8182.
26 S. Fujiwara, Y. Yoshizaki, A. Kuzuya and Y. Ohya, *Acta Biomater.*, 2021, **135**, 318.
27 X. Yang, Q. Ma, G. Xu, L. Yu and J. Ding, *Bioact. Mater.*, 2021, **6**, 4717–4728.
28 L. Yu, W. Xu, W. Shen, L. Cao, Y. Liu, Z. Li and J. Ding, *Acta Biomater.*, 2014, **10**, 1251.
29 B. Jeong, Y. H. Bae, D. S. Lee and S. W. Kim, *Nature*, 1997, **388**, 860.
30 B. Jeong, Y. H. Bae and S. W. Kim, *Colloids Surf., B*, 1999, **16**, 185.
31 B. Jeong, Y. H. Bae and S. W. Kim, *Macromolecules*, 1999, **32**, 7064.
32 B. Jeong, Y. H. Bae and S. W. Kim, *J. Biomed. Mater. Res.*, 2000, **50**, 171.
33 D. S. Lee, M. S. Shim, S. W. Kim, H. Lee, I. Park and T. Chang, *Macromol. Rapid Commun.*, 2001, **22**, 587.
34 Y. J. Kim, S. Choi, J. J. Koh, M. Lee, K. S. Ko and S. W. Kim, *Pharm. Res.*, 2001, **18**, 548.
35 G. M. Zentner, R. Rathi, C. Shih, J. C. MaRea, M. H. Seo, H. Oh, B. G. Rhee, J. Mestecky, Z. Moldoveanu, M. Morgan and S. Weitman, *J. Controlled Release*, 2001, **72**, 203.
36 M. Qiao, D. Chen, X. Ma and Y. Liu, *Int. J. Pharm.*, 2005, **294**, 103.
37 H. Deng, A. Dong, J. Song and X. Chen, *J. Controlled Release*, 2019, **297**, 60.
38 G. Ma, B. Miao and C. Song, *J. Appl. Polym. Sci.*, 2010, **116**, 1985.
39 M. J. Hwang, J. M. Suh, Y. H. Bae, S. W. Kim and B. Jeong, *Biomacromolecules*, 2005, **6**, 885.
40 S. J. Bae, J. M. Suh, Y. S. Sohn, Y. H. Bae, S. W. Kim and B. Jeong, *Macromolecules*, 2005, **38**, 5260.
41 S. J. Bae, M. K. Joo, Y. Jeong, S. W. Kim, Y. K. Lee, Y. S. Sohn and B. Jeong, *Macromolecules*, 2006, **39**, 4873.
42 C. Chen, L. Chen, L. Cao, W. Shen, L. Yu and J. Ding, *RSC Adv.*, 2014, **4**, 8789.
43 L. Yu, Z. Zhang and J. Ding, *Biomacromolecules*, 2011, **12**, 1290.
44 L. Yu, G. Chang, H. Zhang and J. Ding, *J. Polym. Sci., Part A: Polym. Chem.*, 2007, **45**, 1122.
45 Z. Jiang, Y. You, X. Deng and J. Hao, *Polymer*, 2007, **48**, 4786.
46 Z. Jiang, Y. You, Q. Gu, J. Hao and X. Deng, *Macromol. Rapid Commun.*, 2008, **29**, 1264.
47 L. Yu, W. Sheng, D. Yang and J. Ding, *Macromol. Res.*, 2013, **21**, 207.
48 T. Fujiwara, T. Mukose, T. Yamaoka, H. Yamane, S. Sakurai and Y. Kimura, *Macromol. Biosci.*, 2001, **1**, 204.
49 T. Mukose, T. Fujiwara, J. Nakano, I. Taniguchi, M. Miyamoto, Y. Kimura, I. Teraoka and C. W. Lee, *Macromol. Biosci.*, 2004, **4**, 361.
50 Y. Yoshida, A. Takahashi, A. Kuzuya and Y. Ohya, *Polym. J.*, 2014, **46**, 632.
51 K. Takata, K. Kawahara, Y. Yoshida, A. Kuzuya and Y. Ohya, *Polym. J.*, 2017, **49**, 677.
52 Y. Yoshida, K. Takata, H. Takai, K. Kawahara, A. Kuzuya and Y. Ohya, *J. Biomater. Sci., Polym. Ed.*, 2017, **28**, 1427.

53 Y. Yoshida, K. Kawahara, K. Inamoto, S. Mitsumune, S. Ichikawa, A. Kuzuya and Y. Ohya, *ACS Biomater. Sci. Eng.*, 2017, **3**, 56.
54 Y. Ohya, *Polym. J.*, 2019, **51**, 997.
55 I. W. Velthoen, J. van Beek, P. J. Dijkstra and J. Feijen, *React. Funct. Polym.*, 2011, **71**, 245.
56 K. Nagahama, K. Fujiura, S. Enami, T. Ouchi and Y. Ohya, *J. Polym. Sci., Part A: Polym. Chem.*, 2008, **46**, 6317.
57 S. J. Lee, B. R. Han, S. Y. Park, D. K. Han and S. C. Kim, *J. Polym. Sci., Part A: Polym. Chem.*, 2006, **44**, 888.
58 C. Lu, L. Liu, S. R. Guo, Y. Zhang, Z. Li and J. Gu, *Eur. Polym. J.*, 2007, **43**, 1857.
59 Y. J. Jun, K. M. Park, Y. K. Joung, K. D. Park and S. J. Lee, *Macromol. Res.*, 2008, **16**, 704.
60 B. Jeong, L. Q. Wang and A. Gutowska, *Chem. Commun.*, 2001, **16**, 1516.
61 B. Jeong, M. R. Kibbey, J. C. Birnbaum, Y. Y. Won and A. Gutowska, *Macromolecules*, 2000, **33**, 8317.
62 K. Nagahama, Y. Imai, T. Nakayama, J. Ohmura, T. Ouchi and Y. Ohya, *Polymer*, 2009, **50**, 3547.
63 A. Takahashi, M. Umezaki, Y. Yoshida, A. Kuzuya and Y. Ohya, *Polym. Adv. Technol.*, 2014, **25**, 1226.
64 A. Takahashi, M. Umezaki, Y. Yoshida, A. Kuzuya and Y. Ohya, *J. Biomater. Sci., Polym. Ed.*, 2014, **25**, 444.
65 J. Lee, Y. H. Bae, Y. S. Sohn and B. Jeong, *Biomacromolecules*, 2006, **7**, 1729.
66 Y. Yoshida, H. Takai, K. Kawahara, S. Mitsumune, K. Takata, A. Kuzuya and Y. Ohya, *Biomater. Sci.*, 2017, **5**, 1304.
67 J. Luan, S. Cui, J. Wang, W. Shen, L. Yu and J. Ding, *Polym. Chem.*, 2017, **8**, 2586.
68 K. Wu, X. Chen, S. Gu, S. Cui, X. Yang, L. Yu and J. Ding, *Macromolecules*, 2021, **54**, 7421.
69 S. Sasaki, N. Kuwahara, M. Nakata and M. Kaneko, *Polymer*, 1977, **18**, 1027.
70 S. Cui, L. Chen, L. Yu and J. Ding, *Macromolecules*, 2020, **53**, 7726.
71 L. Chen, T. Ci, L. Yu and J. Ding, *Macromolecules*, 2015, **48**, 3662–3671.